

ACCEPTED FOR PUBLICATION IN

Biochimica et Biophysica Acta (2007) vol. 1771, issue # 9, pp. 1226–1234. Epub 2007 Jun 7.

THIS DOCUMENT IS IDENTICAL TO CORRECTED PROOF (FINAL PUBLISHED VERSION)

<http://www.sciencedirect.com/science/article/pii/S1388198107001126>

<http://pubmed.gov/17604219>

Alteration of ganglioside synthesis by GM3 synthase knockout in murine embryonic fibroblasts

Nikolai A. Shevchuk ^{a,d}, Yetrib Hathout ^b, Olga Epifano ^a, Yan Su ^a, Yihui Liu ^a,
Margaret Sutherland ^c, Stephan Ladisch ^{a,d,*}

^a Center for Cancer and Immunology Research, Children's Research Institute,
111 Michigan Avenue, NW, Washington, DC 20010, USA

^b Center for Genetic Medicine, Children's Research Institute, 111
Michigan Avenue, NW, Washington, DC 20010, USA

^c Center for Neuroscience Research, Children's Research Institute, 111
Michigan Avenue, NW, Washington, DC 20010, USA

^d Molecular and Cellular Oncology Program, Institute for Biomedical Sciences, The
George Washington University, Washington, DC, USA

Received 11 April 2007; received in revised form 16 May

2007; accepted 21 May 2007

Available online 7 June 2007

Abbreviations: MEF, murine embryonic fibroblasts; GM3S, GM3 synthase; NAc, N-acetylneuraminic acid; NGc, N-glycolylneuraminic acid; SA, Sialic acid

* Corresponding author. Center for Cancer and Immunology Research, Children's Research Institute, 111 Michigan Avenue, NW, Washington, DC 20010, USA. Tel.: +1 202 884 3898; fax: +1 202 884 3929. E-mail address: sladisch@cnmc.org (S. Ladisch).

Abstract

To probe the functions of membrane gangliosides, the availability of ganglioside-depleted cells would be a valuable resource. To attempt to identify a useful genetic model of ganglioside depletion, we assessed ganglioside metabolism in murine GM3 synthase (GM3S)^{-/-} knockout primary embryonic fibroblasts (MEF), because normal fibroblast gangliosides (GM3, GM2, GM1, and GD1a), all downstream products of GM3S, should be absent. We found that heterozygote MEF (GM3S^{+/-}) did have a 36% reduced content of qualitatively normal gangliosides (7.0±0.8 nmol LBSA/mg cell protein; control: 11±1.6 nmol). However, two unexpected findings characterized the homozygous (GM3^{-/-}) MEF. Despite complete knockout of GM3S, (i) GM3^{-/-} MEF retained substantial ganglioside content (21% of normal or 2.3±1.1 nmol) and (ii) these gangliosides were entirely different from those of wild type MEF by HPTLC. Mass spectrometry identified them as GM1b, GalNAc-GM1b, and GD1α, containing both N-acetyl and N-glycolylneuraminic acid and diverse ceramide structures. All are products of the 0 pathway of ganglioside synthesis, not normally expressed in fibroblasts. The results suggest that complete, but not partial, inhibition of GM3 synthesis results in robust activation of an alternate pathway that may compensate for the complete absence of the products of GM3S.

©2007 Published by Elsevier B.V.

Keywords: Gangliosides; GM3 synthase; Knockout; Mouse embryonic fibroblasts; O-pathway

1. Introduction

Gangliosides are membrane glycosphingolipids containing sialic acid residue(s). They are located predominantly in the outer leaflet of the lipid bilayer with the negatively charged sialic acids extending into the extracellular space. While they are quantitatively a minor component of the lipids present in most mammalian cell membranes, their potential for having important biological functions has intrigued investigators now for many years [1]. Much progress has been made in understanding both normal and abnormal cell ganglioside function, to a large extent through in vitro studies of effects of added exogenous gangliosides. On the other hand, normal functions of endogenous gangliosides remain to be fully elucidated, and little is yet known about cellular mechanisms of action.

Several approaches have been developed to intrinsically alter ganglioside metabolism and thereby endogenous cellular ganglioside content. One is pharmacologic inhibition of ganglioside synthesis. For example, the glucosylceramide synthase inhibitor, PPPP (D-1-threo-1-phenyl-2-hexadecanoylamino-3-pyrrolidino-1-propanol-HCl), effectively depletes cellular gangliosides [2], but it also inhibits the synthesis of the neutral

glycosphingolipids glucosylceramide and lactosylceramide. Ideal would be a small molecule that specifically inhibits ganglioside synthesis such as by targeting GM3 synthase (GM3S), a key enzyme in human and murine extraneural tissue ganglioside synthesis, but such a molecule has yet to be discovered.

A second, recently employed approach is the knockout of glycosyltransferase genes involved in ganglioside synthesis. A number of knockout mice in which these genes have been targeted have been developed (reviewed in [3]). Study of these murine models has revealed apparent functional redundancy among related ganglioside structures. Knockouts affecting only one or another group of gangliosides (such as complex gangliosides) frequently have a only mild effect on phenotype [4,5] and lifespan [6]. At the other extreme is complete knockout of all gangliosides by targeting multiple or upstream genes, which can cause severe neurodegeneration and embryonic lethality [7] or fatality early in life [8].

Here we have attempted to develop and characterize an in vitro cell culture system that would allow study of the effects of complete ganglioside depletion at the cellular level, particularly on the function of cells that are present in peripheral tissues. We used the GM3S knockout mouse, a kind gift of Dr. Richard Proia, to culture embryonic fibroblasts (MEF) for this purpose. We reasoned that these MEF might constitute a valuable model system because all the gangliosides normally found in fibroblasts [9–12] are derived from the product (GM3) of the affected enzyme (GM3S).

We expected to confirm complete or nearly complete ganglioside depletion in the MEF. Contrary to this expectation, while we did document the anticipated absence of GM3 and the normally present A pathway gangliosides, the MEF were not ganglioside-depleted. Rather, significant quantities of qualitatively different gangliosides were found. Consequently, we performed a detailed ganglioside analysis which is the subject of this report.

Our analysis shows that the gangliosides identified reflected substantial activation of the O pathway, normally not expressed in murine fibroblasts. While recently it was suggested (based on their detection in the brains of GM3S^{-/-} mice [6]) that traces of uncharacterized gangliosides detected in GM3S^{-/-} MEF might be gangliosides of the O series [13], they were not identified nor characterized by these authors [13]. Here we have identified and characterized these O series gangliosides in GM3S^{-/-} MEF by mass spectrometry, and revealed their existence in MEF in unexpectedly high concentrations.

2. Materials and methods

2.1. Derivation of mouse embryonic fibroblasts from GM3 synthase KO mice

Two breeding pairs of GM3 synthase knockout mice (C57BL/6 background) were a generous gift of Richard Proia (NIH, Bethesda, MD). Mouse embryonic fibroblasts (MEF) were derived and cultured from GM3S^{+/+}, GM3S^{+/-}, and GM3S^{-/-} 13-day

embryos, obtained by matings of GM3S^{+/-} × GM3S^{+/-} mice, and following the protocol of the WiCell Research Institute. MEF were cultured for 3 passages in T-175 cell culture flasks at 37 °C and 5% CO₂ in DMEM containing 4.5 g/L glucose (BioWhittaker, MD), supplemented with 10% FBS, 2 mM L-glutamine, 0.1 mM non-essential amino acids, and Pen-Strep antibiotic mix (Invitrogen, CA). Then the cells were harvested and frozen in the same medium with 5% DMSO, without antibiotics. All subsequent passages of MEF were in the same medium without antibiotics.

2.2. Genotyping of mice and MEF

Genomic DNA from tails of GM3 synthase knockout mice and mouse embryos was purified and the embryos were genotyped using PCR with two sets of primers as described [6]. Afterwards, established cell clones were regentyped. Genomic DNA was isolated from 5×10^5 cells using QiaAmp DNA Mini Kit (Qiagen) and eluted with 30 μ L of 5 mM Tris-HCl buffer pH 8.5 during the last step of the protocol. 2 μ L of DNA samples were used in 20 μ L PCR reactions using SibGene Taq Polymerase kit (SibGene, MD). Primers 5'-AGCTCAGAGCTATGCTCAGGA-3' and 5'-TAC-CACATCGAACTGGTTGAG-3' were used to detect the wild-type GM3 synthase gene (~400 bp PCR product). Primers 5'-CAATAGATCTGACCCCTATGC-3' and 5'-

GCCTTCTTGACGAGTTCTTCTGAG-3' were used to identify the mutant GM3 synthase allele, yielding a ~300 bp PCR product. Cycling conditions were: 40 cycles; denaturation 94 °C, 1 min; annealing 60 °C, 1 min; extension 72 °C, 1 min.

2.3. Proliferation assays

10⁵ cells/well were seeded in 6-well plates and cultured in DMEM with 4.5 g/L glucose (BioWhitaker, MD), supplemented with 10% FBS, 2 mM L-glutamine, and 0.1 mM non-essential amino acids (Invitrogen, CA). Duplicate wells of each cell type were harvested during log phase growth (days 2 and 4) and counted. Each experiment was performed twice in duplicate and the mean proliferation rate calculated.

2.4. Ganglioside isolation and purification

Total lipid extracts of cell pellets were obtained by extracting the lyophilized starting material twice with chloroform/methanol (1:1, by volume) for 18 h at 4 °C with stirring. Gangliosides were isolated from the lower phase of the dried total lipid extract partitioned in diisopropyl ether/1-butanol/17 mM aqueous NaCl (6:4:5, by volume) [14]. The gangliosides were further purified by Sephadex G-50 gel filtration. HPTLC analysis of gangliosides was performed using 10×20 cm precoated silica gel 60 HPTLC plates (Merck, Darmstadt). The plates were developed in chloroform/methanol/0.25% aqueous CaCl₂·2H₂O (60:40:9, by volume) to separate gangliosides (stained as purple bands

with resorcinol reagent), followed by densitometric ganglioside quantification. For preparative isolation, the ganglioside bands were visualized in iodine vapor, scraped from the HPTLC plate into 1 ml conical glass tubes, extracted from silica using chloroform:methanol:water solution (60:35:8, v/v/v), and dried under vacuum centrifugation using SpeedVac. The residues were redissolved in 20 μ l of acetonitrile:water (1:1, v/v) and analyzed by mass spectrometry.

2.5. Mass spectrometric analysis of MEF gangliosides

0.3 μ L of TLC purified ganglioside solution was mixed with 0.3 μ L of matrix solution (50 mM alpha-cyano-4-hydroxynamic acid in acetonitrile) and spotted on a MALDI plate. Mass spectrometry (MS) and tandem mass spectrometry (MS/MS) analyses were performed on a 4700 ABI TOF-TOF mass spectrometer (Applied Biosystems, Foster City, CA) equipped with Nd:YAG 200 Hz laser. The instrument was operated with delayed extraction in reflectron negative ion mode. A mixture of standard peptides (4700 Cal Mix from Applied Biosystems, Foster City, CA) was used to externally calibrate the instrument. Standard gangliosides (bovine GM1 and GD1a; Matreya) constituted additional controls for mass accuracy and for MS/MS fragmentation patterns.

3. Results

3.1. *GM3S* knockout murine embryonic fibroblasts

13.5-day-old embryos from the cross of *GM3S*^{+/-} (heterozygous) parents were harvested and DNA analyzed by PCR. A number of MEF clones of each genotype (*GM3S* wild type, heterozygote and homozygote knockout) were successfully derived. Their genotype was confirmed by PCR, and representative PCR genotyping results are shown in [Fig. 1A](#). There were no discernable differences in MEF cell morphology among the three genotypes ([Fig. 1B](#)) and the rates of proliferation were similar as well (wild type and heterozygote MEF increased to 2.0-fold the initial cell number in 48 h, whereas *GM3S*^{-/-} MEF increased to 1.85 fold, $p < 0.05$). Since an altered cell proliferation rate by cell counting was not observed, slightly increased thymidine incorporation (not shown), which parallels a similar increase in the MTT assay in these cells [\[13\]](#), may be due to altered membrane transport of the reagents thymidine and MTT, possibly because of membrane lipid modifications.

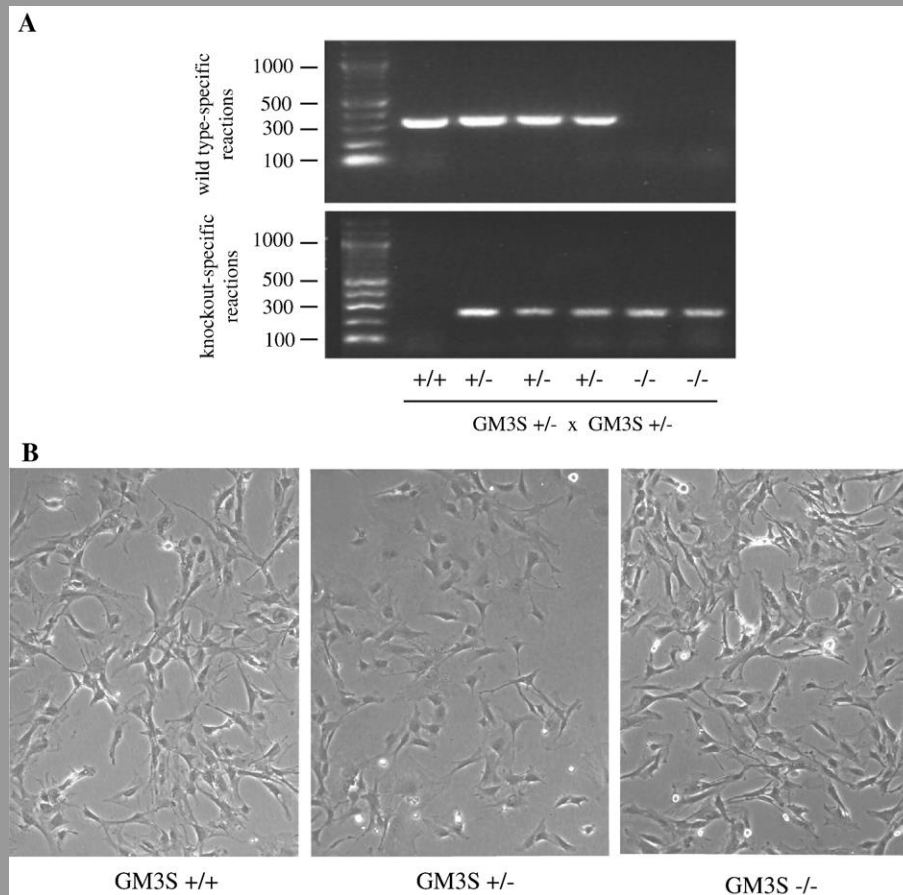


Fig. 1. Genotypic and phenotypic characterization of MEF. (A) PCR analysis of MEF obtained from one litter (six embryos) of a GM3S^{+/-} × GM3S^{+/-} mating. Primers 5'-AGCTCAGAGCTATGCTCAGGA-3' and 5'-TACCACATCGAACTGGTTGAG-3' (upper panel) yielded a ~400 bp PCR product used to detect the wild-type copy of GM3 synthase gene. Primers 5'-CAATAGATCTGACCCCTATGC-3' and 5'-TCGCCTTCTTGACGAGTTCTTCTGAG-3' (lower panel) yielded a ~300 bp PCR product used to detect the mutant GM3 synthase allele. The gels were 1.6% agarose stained with ethidium bromide, with a 100-bp DNA ladder (New England Biolabs) as markers. (B) Cell morphology of GM3S^{-/-}, ^{+/-}, and wild type MEF. Photomicrographs were taken using a ZEISS Axiovert 135 microscope (10×/0.25 objective).

3.2. Ganglioside analysis of GM3 synthase-deficient MEF

HPTLC densitometry revealed a wild type MEF ganglioside content of 11 ± 1.6 nmol LBSA/mg protein (mean \pm S.D., Fig. 2A, B). There was a 36% reduction in total gangliosides, to 7.0 ± 0.8 nmol LBSA/mg protein, in the heterozygote cells (Fig. 2A, B). Somewhat surprisingly, the GM3S^{-/-} MEF retained a substantial ganglioside content (2.3 ± 1.1 nmol LBSA/mg protein) but with a completely different HPTLC profile from that of wild type or heterozygote cells (Fig. 2A). We previously identified the major gangliosides of normal wild type murine fibroblasts [12]. They are GD1a, GM1, GM2, and GM3, and appear as doublets because of the existence of multiple different ceramide species of each ganglioside. In GM3S^{+/-} MEF, GD1a comprised 60% (and the other three gangliosides together 40%) of the total gangliosides. Qualitatively, heterozygote MEFs had an identical ganglioside pattern and proportionally identical expression of these gangliosides to normal MEFs. These findings indicate preservation of at least partial enzyme activity of GM3S, in the MEF heterozygous for the allele. The HPTLC of GM3S^{-/-} MEF gangliosides, however, was completely different from that of GM3S^{+/-} and GM3S^{+/+} MEF. Two sets of bands, with 5 distinct and several faint bands, migrating very differently from those of GM1 and GD1a seen in the normal and heterozygote MEF, are visible (Fig. 2A and C).

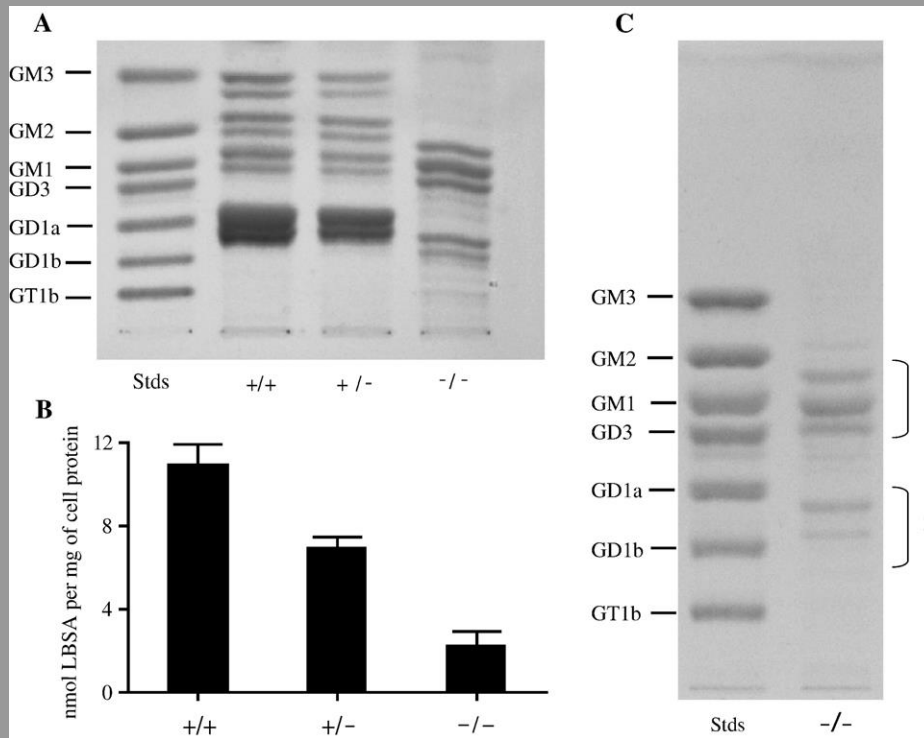


Fig. 2. HPTLC analysis of MEF gangliosides from GM3 synthase wild type (GM3S^{+/+}), heterozygous (GM3S^{+/-}), and homozygous (GM3S^{-/-}) knockout mice. (A) HPTLC. Each lane contains total gangliosides isolated from 8×10^6 cells of the genotype indicated. Stds: bovine brain standard gangliosides. (B) Quantification by HPTLC densitometry. Each bar represents the mean \pm S.D. of three separate samples, expressed as nmol lipid-bound sialic acid (LBSA)/mg cell protein. (C) Preparative HPTLC for mass spectrometry. Gangliosides of 6×10^7 GM3S^{-/-} MEF were scraped into fraction 1 (upper three bands) and fraction 2 (lower two bands) and extracted from the silica with chloroform:methanol:water (60:35:8, v/v/v) for analysis by MALDI-TOF. Bovine standards are shown on the left. The major ganglioside band of heterozygote (GM3S^{+/-}) MEF, which migrated as GD1a in panel A, was also isolated for analysis.

As a result of these findings of incomplete ganglioside depletion but replacement with a different ganglioside pattern, we isolated the gangliosides from GM3S^{-/-} and GM3S^{+/-} MEF for further analysis. The major gangliosides were separated by preparative HPTLC. Two ganglioside fractions, 1 and 2 in Fig. 2C, were extracted from the preparative HPTLC of GM3S^{-/-} MEF. We also isolated (Fig. 2C), as was the major band from the HPTLC of the heterozygote, GM3S^{+/-}, MEF. These gangliosides were characterized by mass spectrometry.

3.3. Mass spectrometric identification of gangliosides in GM3^{-/-} and GM3^{+/-} MEF

Fig. 3A, C, and E show the MALDI-TOF mass fingerprints of GM3S^{-/-} fraction 1, GM3S^{-/-} fraction 2, and the major GM3S^{+/-} ganglioside, respectively. Major peaks in each MS were subjected to MS/MS analysis and their fragmentation patterns compared to those of standard brain gangliosides and of mouse gangliosides [15–17]. Representative MS/MS spectra are shown in Fig. 3B, D, and F. They characterize a major ganglioside of GM3S^{-/-} MEF ganglioside fraction 1 (Fig. 3B), GM3S^{-/-} MEF ganglioside fraction 2 (Fig. 3D), and the major GM3S^{+/-} MEF ganglioside (Fig. 3F).

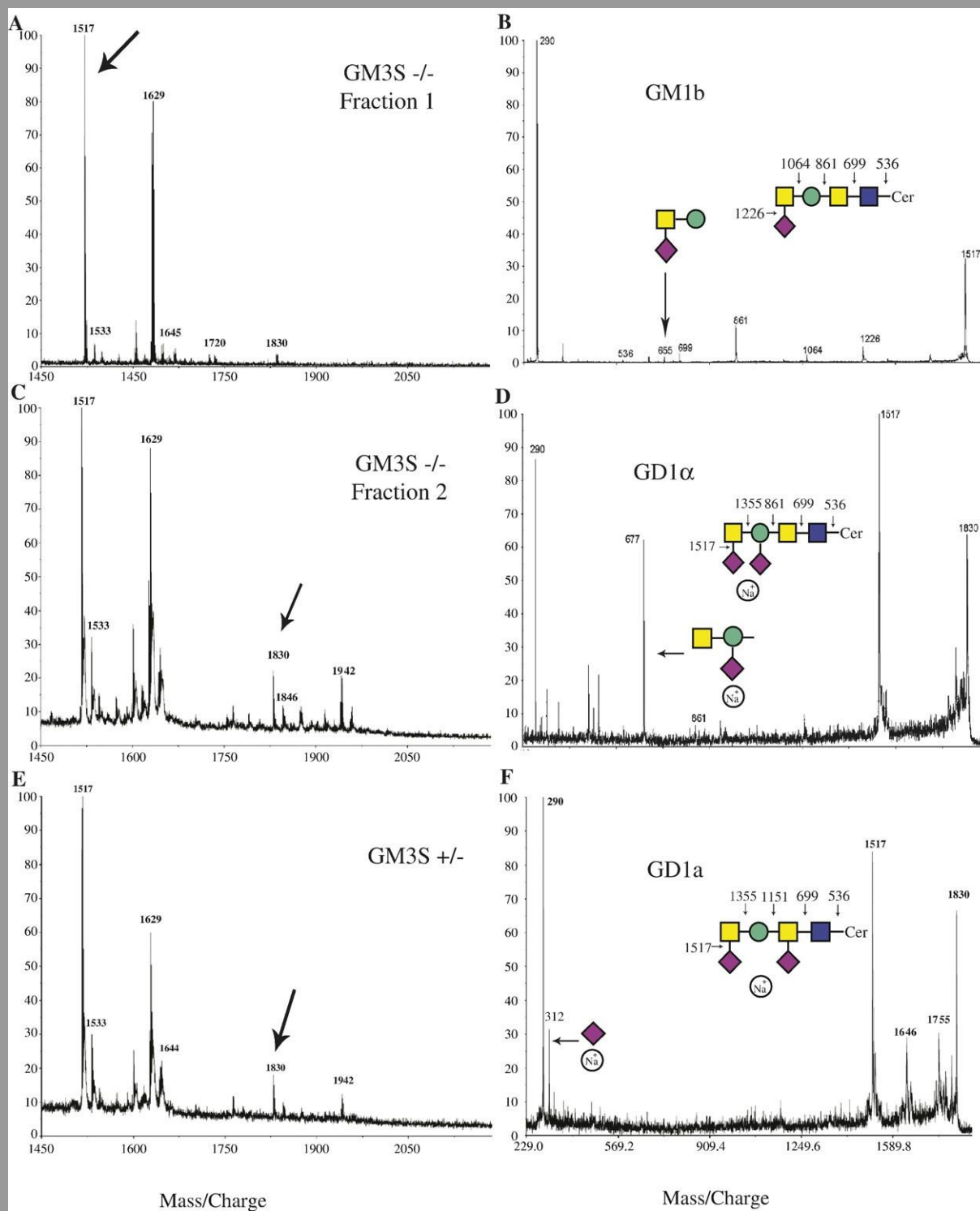


Fig. 3. Mass spectrometric analysis of MEF gangliosides. Panels A, C, and E represent reflectron negative ion detection MALDI-TOF mass spectra of GM3S^{-/-} fraction 1 (panel A), fraction 2 (panel C), and the GM3S^{+/-} major band, migrating as GD1a (panel E). Panels B, D, and F are representative MS/MS analyses by reflectron negative ion detection MALDI-TOF tandem mass spectrometry of the selected major molecular ion indicated by the arrow in panels A, C, and E, respectively. (A) Fraction 1 contained major molecular ions 1517, 1629, and 1627 that are gangliosides GM1b d18:1-C16:0, d18:1-C24:0, and d18:1-C24:1, respectively. Molecular ions 1720, 1832, and 1830 represent gangliosides GalNAc-GM1b of the same three ceramide structures. (B) Tandem MS fragmentation pattern and identification of ganglioside GM1b. (C) fraction 2 contained molecular ions 1830, 1942 and 1940, which represent gangliosides GD1 α d18:1-C16:0, d18:1-C24:0, and d18:1-C24:1 respectively, as well as 1846 (d18:1-C16:0 GD1 α with N-glycolylneuraminic acid). (D) Tandem MS fragmentation pattern and identification of ganglioside GD1 α . (E) The major peaks of the major GM3S^{+/-} band are molecular ions 1830, 1942 and 1940, consistent with ganglioside GD1a d18:1-C16:0, d18:1-C24:0, GD1a d18:1-C24:1 respectively. (F) Tandem MS fragmentation pattern and identification of ganglioside GD1a in panel E.

Mass spectrometry of fraction 1 (Fig. 3A), which contained the predominant bands in GM3S^{-/-} MEF (70% of the total gangliosides), showed a prominent set of peaks at m/z 1517, 1627, and 1629. There were also sets of peaks at m/z 1720, 1830, and 1832, and at m/z 1533, and 1643/1645. Fig. 3B shows the MS/MS data obtained for the major peak at m/z 1517 detected in fraction 1. Most of the observed ions corresponded to fragmentation occurring in the carbohydrate chain-sequential loss of monosaccharides and as a characteristic fragment at m/z 655. A prominent recognizable fragment at m/z 290, indicative of the presence of a terminal sialic (N-acetylneuraminic acid, NAc) acid (SA) residue in the carbohydrate chain is also seen in the spectrum. Comparison of the MS/MS data of the peaks at 1517, 1627 and 1629 showed identical carbohydrate fragmentation patterns, consistent with them being GM1b containing d18:1-C16:0, d18:1-C24:1, and d18:1-C24:0 ceramide moieties, respectively. The minor peaks at m/z 1533,

1643, and 1645 were consistent with GM1b containing N-glycolylneuraminic acid (NGc) rather than NAc [17], as confirmed by MS/MS (not shown), with the same ceramide composition as the major GM1b species. The set of peaks at m/z 1720, 1830, and 1832 are consistent with the structure GalNAc–GM1b (although GlcNAc–GM1b cannot be excluded by the mass spectrometric findings alone). Until now, only GalNAc–GM1b has been identified as an 0 pathway ganglioside, present in murine macrophage-like tumor cells [18]. The ceramide moieties once again are identical to those of the major ganglioside GM1b. Fraction 1 of the homozygote GM3S^{-/-} MEF thus contains three variants of GM1b, namely NAcGM1b and NGcGM1b, and GalNAc–GM1b, each with at least three distinct ceramide moieties. All are structures of the 0 pathway.

Fraction 2 (Fig. 3C), comprising about 30% of the total GM3S^{-/-} MEF gangliosides, contained the gangliosides more complex than those in fraction 1. Beginning with the higher mass peaks, there was a set of prominent peaks at m/z 1830, 1940, and 1942, and a peak at 1846. Corresponding lower mass peaks were found at 1517, 1627, and 1629, and at 1533. Tandem mass spectrometry (MS/MS) for the peak at m/z 1830 is shown in Fig. 3D. The carbohydrate fragmentation pattern is consistent with the sodium adduct of the hypothesized structure, GD1 α , with a fragment ion indicative of the presence of sialic acid (SA) detected at m/z 290. Clearly distinguishing this species from GD1a is a distinctive fragment ion at m/z 677. This fragment was seen in the MS/MS spectra of all suspected GD1 α species, but not detected in the MS/MS spectrum of GD1a

ganglioside standard (not shown), and corresponds to the $[\text{Gal}+\text{GalNAc} + \text{SA} + \text{Na}^+]^-$ moiety. The spectrum also contains a prominent fragment ion at m/z 1517. This would be consistent with the loss of $[\text{SA} + \text{Na}^+]$ from the parent ion at m/z 1830. There is precedent for the detection of sodium adducts by MALDI-TOF ganglioside analysis; it has been shown previously [16] that A series gangliosides, including the disialo-ganglioside GD1a (of which GD1 α , is an isomer) tend to form adducts with one ion of sodium. Thus we concluded that the peaks at m/z 1830, 1940, and 1942 corresponded to GD1 α , with ceramide moieties d18:1-C16:0, d18:1-C24:1, and d18:1-C24:0, respectively. The minor peak at 1846 is consistent with a GD1 α structure containing one N-glycolylneuraminic (and one N-acetylneuraminic) acid residue, and the peak at 1533 corresponding to its fragment $[\text{M-N-glycolylneuraminic acid-Na}^+]^-$. The possibility that the peak at 1830 in fraction 2 and the minor peak at m/z 1830 in fraction 1 represent identical ganglioside molecular species was excluded by the ms/ms (not shown) of the 1830 peak of fraction 1. It had an entirely different fragmentation pattern; there was no peak at m/z 1517 and therefore no terminal sialic acid, and no peak at m/z 677.

MS/MS analysis of the other major peaks of fraction 2, m/z 1517 and 1627/1629, produced the same prominent peak at m/z 677 that was seen in the MS/MS spectrum of GD1 α (Fig. 3D), but not seen in the MS/MS of GM1b (Fig. 3B). This suggests that the peaks at m/z 1517 and 1627/1629 in Fig. 3C are not native GM1b (which, found in fraction 1, migrates further on HPTLC than the disialogangliosides) but the result of in

source fragmentation of GD1 α , which tends to easily lose a sialic acid moiety during MALDI-TOF analysis [16].

We also analyzed the major ganglioside of the heterozygote GM3S $^{+/-}$ MEF (Fig. 3E). This ganglioside migrated on HPTLC similar to GD1a, and the HPTLC pattern of the GM3S $^{+/-}$ MEF was identical to that of wild type cells, known to contain GD1a as a major component. Prominent peaks are seen again at m/z 1830 and 1940/42, and at m/z 1517 and 1629. The MS/MS fragmentation pattern of the species at m/z 1830 (Fig. 3F) is consistent with the structure being a sodium adduct of GD1a. Importantly, the discriminating fragment at m/z 677, present in GD1 α (Fig. 3D) was not found in GD1a standard ganglioside nor in the heterozygote ganglioside sample (Fig. 3F), which does contain a prominent fragment ion at m/z 1517, which would be consistent with loss of [SA+ Na $^{+}$] from the parent ion at m/z 1830, and also a fragment at m/z 312, consistent with a [SA +NA $^{+}$] $^{-}$ fragment. Thus, the major GM3S $^{+/-}$ ganglioside was identified as GD1a, with the same ceramide moieties as those of the abnormally expressed 0 series gangliosides above.

In summary (Fig. 4), GM3S $^{-/-}$ MEF express mainly sialic acid-containing GM1b, GalNAc-GM1b, and GD1 α with trace amounts of N-glycolylneuraminic acid-containing GM1b and GD1 α . In contrast, the heterozygous GM3S $^{+/-+/-}$ MEF expressed, at a reduced level, the normal MEF gangliosides including GD1a, and smaller quantities of GM3, GM2, and GM1a. Importantly, they did not express GD1 α , which is the analogous

0 pathway ganglioside to GD1a. Thus there is a clear and complete qualitative distinction between the ganglioside composition of GM3S^{-/-} MEF, and wild type and heterozygote cells. This distinction might not have been noticed by ganglioside quantification alone, would have shown only a gradual reduction in ganglioside content with graded knockout of GM3S enzyme activity.

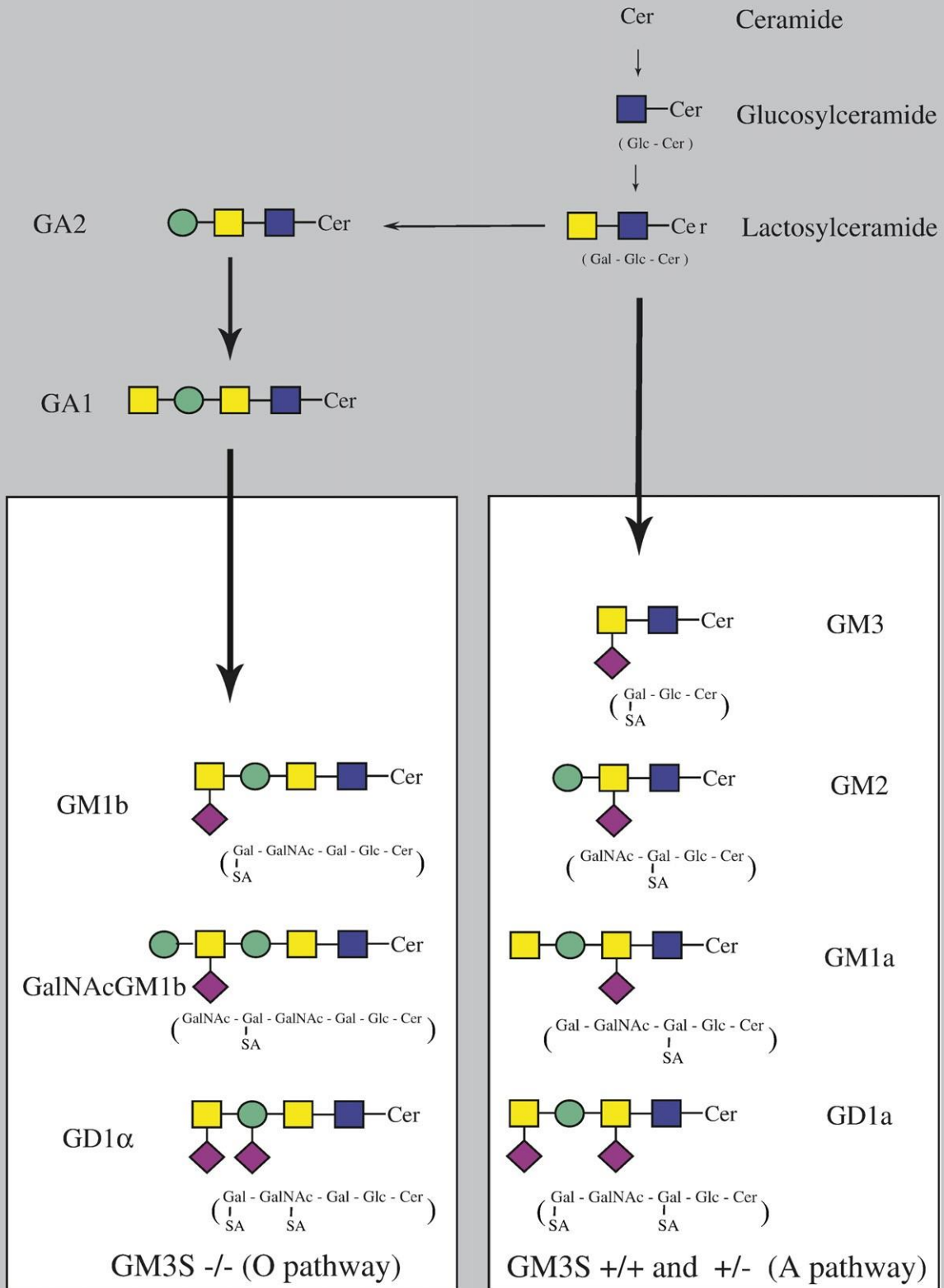


Fig. 4. Schematic summary of MEF ganglioside synthesis in GM3 synthase wild type (GM3S^{+/+}), heterozygous (GM3S^{+/-}), and homozygous (GM3S^{-/-} knockout) mice. Highlighted areas show gangliosides that are expressed in the respective MEF.

4. Discussion

Models to study alterations in ganglioside metabolism are of interest because of their potential utility, when ganglioside depletion can be achieved, in dissecting mechanisms of the biological activities of these molecules. An ideal model would be genetically altered to express a single gene defect, reducing the risk of multiple effects that can be associated with pharmacological strategies. In the case of ganglioside expression, the optimal manipulation would be a knockout in which all normally present gangliosides are derivatives of the targeted enzyme. In undertaking the present study, this was presumed to be the case for MEF of the GM3S knockout mouse, because normal MEF gangliosides are all derived from GM3.

Thus we embarked on a careful study of ganglioside expression in GM3S MEF. The approximate 40% reduction in the level of gangliosides in the GM3S^{+/-} MEF, compared to wild type MEF, although not predicted, was not unexpected. However, the maintenance of fully one fifth of the normal level of gangliosides in the complete GM3S knockout was unexpected, as was the ganglioside pattern: This substantial residual ganglioside content of the knockout MEF had a completely different HPTLC pattern from that of wild type (and of GM3S^{+/-}) MEF. This unusual complement of gangliosides

consisted entirely of gangliosides of the 0 pathway (GM1b, GalNAcGM1b, and GD1 α). Finally, these findings are not developmentally restricted (e.g., to embryonic fibroblasts), because we have observed identical changes in ganglioside metabolism in fibroblasts of from young adult GM3S $^{-/-}$ mice (unpublished results).

Where are 0 pathway gangliosides found? Normally, they are present in low concentrations in brain, both human and mouse. They have not been detected at all in normal fibroblasts. They are the major or exclusive gangliosides of some murine lymphomas [15] and have been detected in macrophage-like tumor cells [18], as well as in normal mouse lymphocytes and lymph nodes [19], suggesting that they are most commonly expressed in cells of the immune system in mice. The significance of the detection 0 pathway gangliosides in normal mouse brain [20] is that their prominence in GM3S $^{-/-}$ knockout mouse brain [6], where they quantitatively replace the normal brain gangliosides (e.g., GM1, GD1a, GD1b, GT1b), is therefore consistent with the further activation of an enzyme pathway (Fig. 4) that is already operational even in the face of otherwise normal (i.e., active GM3S) ganglioside metabolism in that tissue.

However, because these gangliosides are not expressed in normal fibroblasts, we thought that it would be unlikely for them to be expressed in the GM3S $^{-/-}$ MEF, in contrast to Hashiramoto et al [13], who suggested that the trace amounts of unidentified gangliosides they detected in GM3S $^{-/-}$ fibroblasts may correspond to 0-series gangliosides because these were expressed in the brains of GM3S $^{-/-}$ mice. However, they

detected only traces of gangliosides in GM3S^{-/-} MEF, did not structurally characterize or identify them, and did not detect any gangliosides in other peripheral tissues (muscle and adipose tissue) of this mouse [6]. Thus we were surprised to find substantial amounts of these gangliosides in GM3S^{-/-} MEF. That 0 pathway gangliosides completely replaced the normal gangliosides in GM3S^{-/-} MEF indicated that complete knockout resulted in alternate pathway activation. However, since a switch did not occur in the GM3S^{+/-} MEF, it means that the 0 pathway is only activated in MEF when the knockout was complete (homozygous GM3S^{-/-}). This contrasts to brain, in which minor expression of this pathway already coexists with normal GM3S activity in normal brain ganglioside expression, resulting in simultaneous expression of gangliosides of both pathways.

What are possible causes of the shift to the 0 pathway in GM3S^{-/-} MEF? A number of different mechanisms have been proposed (reviewed in [21]). They include that by preventing anabolism of lactosylceramide to GM3 by GM3S, metabolism of lactosylceramide to asialo-GM2 is accelerated (Fig. 4), overcoming the relative enzyme kinetics that normally favor flow into the GM3S pathway. Another possibility is that the products of GM3S might be inhibitory to asialoGM2 synthesis, so that in the absence of these products of GM3S (i.e., in GM3S^{-/-} mice) asialoGM2 synthase might be activated. A third is that the absence of GM3 synthase causes disruption of a complex of

the three sequential enzymes, lactosylceramide synthase, GM3 synthase, and GD3 synthase, that were identified as a complex by Giraudo and Maccioni [22], and that this disruption shifts synthesis into the O pathway. Our observations add a constraint to possible mechanisms, at least in fibroblasts (in contrast to brain): Since we did not observe any transition to the O pathway in heterozygote cells, it seems that either a substantial increase in the amount of lactosylceramide (the substrate) or a complete absence of GM3 and/or A pathway gangliosides (potential O pathway enzyme inhibitors) must be required for the O-pathway to become activated. Further studies will be needed to pinpoint the mechanism(s) that underlie the switch to O pathway ganglioside synthesis, but because the switch is absolute and complete in these GM3S^{-/-} MEF, they should constitute a valuable model system for developing more complete understanding of the control of the metabolic pathways of ganglioside synthesis.

The absence of gross defects in cell morphology and growth characteristics of GM3S^{-/-} MEF suggests that to the extent that gangliosides play a role in determining normal cell physiology, the O pathway gangliosides i.e., GM1b, GalNacGM1b, and GD1 α , may substitute for normal functions of major gangliosides of the A and B pathways, since GM3S knockout mice show almost normal development and lifespan [6], whereas complete ganglioside knockout mice die early [3]. Recent preliminary findings are consistent with this thought, in that fibroblast EGF-induced EGFR activation and proliferation, which in other studies [12,23] have been shown to be particularly sensitive

to inhibition by ganglioside depletion of the fibroblast cell membrane, appear to be normal in the GM3S^{-/-} cells (unpublished). Of course, this does not exclude the possibility that other subtle defects resulting from the absence of the normal gangliosides in these MEFs remain to be discovered. For example, an abnormality (defective calcium regulation) in the apparently normal cerebellar granular neurons of mice lacking complex gangliosides because of GM2/GD2 synthase knockout became evident in vitro only upon challenge with high intracellular calcium [24]. Our findings do raise the question of whether some well-characterized biological properties of GM3S^{-/-} mice, such as increased insulin sensitivity of muscle [6], and enhanced MAPK signaling in MEF [13], may at least in part be due to the replacement of the major normal gangliosides by those of the 0 pathway. Interestingly, knockout of glucosylceramide synthase [7] or both GM3 synthase and GM2 synthase [8], thus preventing production of any gangliosides of either the 0 or major pathways, is lethal. This further supports the speculation that the presence of 0 pathway gangliosides in the GM3S^{-/-} mouse may indeed substitute for normal functions of major gangliosides and compensate for their absence in maintaining a relatively mildly abnormal phenotype in GMS knockout mice.

Acknowledgements

We are grateful to Dr. Richard Proia for providing the GM3S knockout mice, to Meena Rajagopal for performing the mass spectrometry, and to Arlene Gendron for preparation of the manuscript. This work was supported by NIH grant RO1 CA61010 (SL).

References

- [1] S. Hakomori, Structure, organization, and function of glycosphingolipids in membrane, *Curr. Opin. Hematol.* 10 (2003) 16–24.
- [2] A. Abe, N.S. Radin, J.A. Shayman, L.L. Wotring, R.E. Zipkin, R. Sivakumar, J.M. Ruggieri, K.G. Carson, B. Ganem, Structural and stereo-chemical studies of potent inhibitors of glucosylceramide synthase and tumor cell growth, *J. Lipid Res.* 36 (1995) 611–621.
- [3] R.L. Proia, Glycosphingolipid functions: insights from engineered mouse models, *Philos. Trans. R. Soc. Lond., B Biol. Sci.* 358 (2003) 879–883.
- [4] K.A. Sheikh, J. Sun, Y. Liu, H. Kawai, T.O. Crawford, R.L. Proia, J.W. Griffin, R.L. Schnaar, Mice lacking complex gangliosides develop Wallerian degeneration and myelination defects, *Proc. Natl. Acad. Sci. U. S. A.* 96 (1999) 7532–7537.

- [5] M. Inoue, Y. Fujii, K. Furukawa, M. Okada, K. Okumura, T. Hayakawa, K. Furukawa, Y. Sugiura, Refractory skin injury in complex knock-out mice expressing only the GM3 ganglioside, *J. Biol. Chem.* 277 (2002) 29881–29888.
- [6] T. Yamashita, A. Hashiramoto, M. Haluzik, H. Mizukami, S. Beck, A. Norton, M. Kono, S. Tsuji, J.L. Daniotti, N. Werth, R. Sandhoff, K. Sandhoff, R.L. Proia, Enhanced insulin sensitivity in mice lacking ganglioside GM3, *Proc. Natl. Acad. Sci. U. S. A.* 100 (2003) 3445–3449.
- [7] T. Yamashita, R. Wada, T. Sasaki, C. Deng, U. Bierfreund, K. Sandhoff, R.L. Proia, A vital role for glycosphingolipid synthesis during development and differentiation, *Proc. Natl. Acad. Sci. U. S. A.* 96 (1999) 9142–9147.
- [8] T. Yamashita, Y.P. Wu, R. Sandhoff, N. Werth, H. Mizukami, J.M. Ellis, J.L. Dupree, R. Geyer, K. Sandhoff, R.L. Proia, Interruption of ganglioside synthesis produces central nervous system degeneration and altered axon–glial interactions, *Proc. Natl. Acad. Sci. U. S. A.* 102 (2005) 2725–2730.
- [9] C.M. Andrade, V.M. Trindade, C.C. Cardoso, A.L. Ziulkoski, L.C. Trugo, R.M. Guaragna, R. Borojevic, F.C. Guma, Changes of sphingolipid species in the phenotype conversion from myofibroblasts to lipocytes in hepatic stellate cells, *J. Cell. Biochem.* 88 (2003) 533–544.
- [10] H. Bai, J. Orlando, T.N. Seyfried, Altered ganglioside composition in virally transformed rat embryo fibroblasts, *Biochim. Biophys. Acta* 1136 (1992) 23–27.

- [11] A.V. Komleva, N.V. Prokazova, N.D. Gabrielyan, D.N. Mukhin, L.N. Kashnikova, N.D. Zvezdina, L.E. Martinova, A.F. Panasyuk, Phospholipids and glycosphingolipids in cultured skin fibroblasts from patients with progressive systemic sclerosis (scleroderma), *Clin. Exp. Rheumatol.* 13 (1995) 581–588.
- [12] R. Li, J. Manela, Y. Kong, S. Ladisch, Cellular gangliosides promote growth factor-induced proliferation of fibroblasts, *J. Biol. Chem.* 275 (2000) 34213–34223.
- [13] A. Hashiramoto, H. Mizukami, T. Yamashita, Ganglioside GM3 promotes cell migration by regulating MAPK and c-Fos/AP-1, *Oncogene* 25 (2006) 3948–3955.
- [14] S. Ladisch, B. Gillard, A solvent partition method for microscale ganglioside purification, *Anal. Biochem.* 146 (1985) 220–231.
- [15] R. Li, D. Gage, S. Ladisch, Biosynthesis and shedding of murine lymphoma gangliosides, *Biochim. Biophys. Acta* 1170 (1993) 283–290.
- [16] E. Sugiyama, A. Hara, K. Uemura, T. Taketomi, Application of matrix-assisted laser desorption ionization time-of-flight mass spectrometry with delayed ion extraction to ganglioside analyses, *Glycobiology* 7 (1997) 719–724.
- [17] H.C. Yohe, S. Ye, B.B. Reinhold, V.N. Reinhold, Structural characterization of the disialogangliosides of murine peritoneal macrophages, *Glycobiology* 7 (1997) 1215–1227.

- [18] H.C. Yohe, L.J. Macala, G. Giordano, W.J. McMurray, GM1b and GM1b– GalNAc: major gangliosides of murine-derived macrophage-like WEHI-3 cells, *Biochim. Biophys. Acta* 1109 (1992) 210–217.
- [19] A. Marusic, A. Markotic, N. Kovacic, J. Muthing, Expression of glycosphingolipids in lymph nodes of mice lacking TNF receptor 1: biochemical and flow cytometry analysis, *Carbohydr. Res.* 339 (2004) 77–86.
- [20] S. Furuya, F. Irie, T. Hashikawa, K. Nakazawa, A. Kozakai, A. Hasegawa, K. Sudo, Y. Hirabayashi, Ganglioside GD1 alpha in cerebellar Purkinje cells. Its specific absence in mouse mutants with Purkinje cell abnormality and altered immunoreactivity in response to conjunctive stimuli causing long-term desensitization, *J. Biol. Chem.* 269 (1994) 32418–32425.
- [21] T. Kolter, R.L. Proia, K. Sandhoff, Combinatorial ganglioside biosynthesis, *J. Biol. Chem.* 277 (2002) 25859–25862.
- [22] C.G. Giraud, H.J. Maccioni, Ganglioside glycosyltransferases organize in distinct multienzyme complexes in CHO-K1 cells, *J. Biol. Chem.* 278 (2003) 40262–40271.
- [23] R. Li, Y. Liu, S. Ladisch, Enhancement of epidermal growth factor signaling and activation of SRC kinase by gangliosides, *J. Biol. Chem.* 276 (2001) 42782–42792.

- [24] G. Wu, X. Xie, Z.H. Lu, R.W. Ledeen, Cerebellar neurons lacking complex gangliosides degenerate in the presence of depolarizing levels of potassium, *Proc. Natl. Acad. Sci. U. S. A.* 98 (2001) 307–312.